analytical chemistry

Technical Note

pubs.acs.org/ac

Untargeted Profiling of Tracer-Derived Metabolites Using Stable Isotopic Labeling and Fast Polarity-Switching LC−ESI-HRMS

Bernhard Kluger,[†,¶] Christoph Bueschl,[†,¶] Nora Neumann,[†] Romana Stückler,[‡] Maria Doppler,[†] Alexander W. Chassy,[§] Andrew L. Waterhouse,[§] Justyna Rechthaler,[∥] Niklas Kampleitner,[∥] Gerhard G. Thallinger,[⊥,#] Gerhard Adam,[‡] Rudolf Krska,[†] and Rainer Schuhmacher*[,†]

[†]Center for Analytical Chemistry, Department for Agrobiotechnology (IFA-Tulln), University of Natural Resources and Life Sciences Vienna (BOKU), Konrad-Lorenz-Strasse 20, 3430 Tulln, Austria

[‡]Department of Applied Genetics and Cell Biology, University of Natural Resources and Life Sciences Vienna (BOKU), Konrad-Lorenz-Strasse 24, 3430 Tulln, Austria

[§]Department of Viticulture and Enology, University of California Davis, Davis, California 95616, United States

[∥]University of Applied Sciences Wr. Neustadt, Degree Programme Biotechnical Processes (FHWN-Tulln), Konrad Lorenz Strasse 10, 3430 Tulln, Austria

[⊥]Bioinformatics Group, Institute for Knowledge Discovery, Graz University of Technology, Petersgasse 14, 8010, Graz, Austria

[#]BioTechMed OMICS Center Graz, Stiftingtalstraße 24, 8010, Graz, Austria

Supporting Information

ABSTRACT: An untargeted metabolomics workflow for the detection of metabolites derived from endogenous or exogenous tracer substances is presented. To this end, a recently developed stable isotope-assisted LC−HRMS-based metabolomics workflow for the global annotation of biological samples has been further developed and extended. For untargeted detection of metabolites arising from labeled tracer substances, isotope pattern recognition has been adjusted to account for nonlabeled moieties conjugated to the native and labeled tracer molecules. Furthermore, the workflow has been extended by (i) an optional ion intensity ratio check, (ii) the automated combination of positive and negative ionization mode mass spectra derived from fast polarity switching, and (iii) metabolic feature annotation. These extensions enable the automated, unbiased, and global detection of tracer-derived metabolites in complex biological samples. The workflow is demonstrated with the metabolism of $^{13}C_9$-phenylalanine in wheat cell suspension cultures in the presence of the mycotoxin deoxynivalenol (DON). In total, 341 metabolic features (150 in positive and 191 in negative ionization mode) corresponding to 139 metabolites were detected. The benefit of fast polarity switching was evident, with 32 and 58 of these metabolites having exclusively been detected in the positive and negative modes, respectively. Moreover, for 19 of the remaining 49 phenylalanine-derived metabolites, the assignment of ion species and, thus, molecular weight was possible only by the use of complementary features of the two ion polarity modes. Statistical evaluation showed that treatment with DON increased or decreased the abundances of many detected metabolites.

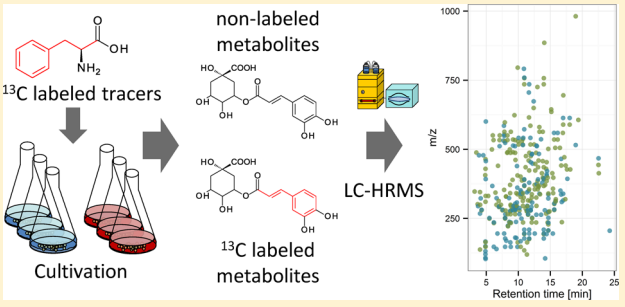

Untargeted metabolomics approaches probe the entire metabolic space of a biological system (e.g., cells or whole organism). This can be realized by trying to measure as many metabolites as possible or alternatively by searching for those metabolites that arise from either exogenous or endogenous substances such as toxins, drugs, or sugars and amino acids, respectively. The screening of such metabolites in LC−HRMS data is rather straightforward when performed in (a) a targeted way with positive lists of putative biotransformation products (e.g., Levsen et al.,[1] Sandermann[2]). In contrast, untargeted approaches are usually more challenging and aim at the detection of known and unknown metabolic products by (b) background subtraction and/or statistical investigation (e.g., Zhang et al.[3]) or (c) isotopic labeling, including stable isotopic labeling (SIL)-assisted approaches. Although the search according to approach a is limited to the subset of predicted, putative tracer derived conjugates (e.g., sugars, amino acids, small peptides) or degradation products known from literature and previous approaches, approach b also enables detecting previously unknown metabolites, but also requires more sophisticated data processing than approach a. Furthermore, the latter approach is prone to detect non-tracer-related metabolites, significantly differing between the investigated

Received: September 2, 2014
Accepted: November 5, 2014
Published: November 5, 2014

sample types. In contrast, approach c provides an easy way to detect both known and unknown tracer-derived metabolites and has the advantage over both a and b that the detected metabolites can be linked to the studied tracer substance (e.g., Baillie,[4] Iglesias et al.[5]).

To avoid the use of radioisotopes, SIL-assisted metabolism studies use stable isotope (e.g., ^{13}C, ^{15}N, or ^{34}S)-enriched tracers and assume that biological systems metabolize native and labeled variants of a supplied tracer nearly equally.[6] Cabaret and colleagues[7] studied U-^{13}C sterigmatocystin in porcine tracheal epithelial cells, and Li and colleagues[8] utilized deuterium labeling together with a principal component analysis guided approach to detect novel metabolites of the drug tempol.

For GC/MS-based, untargeted tracer metabolism studies, Hiller and colleagues[9] presented the NTFD (nontargeted tracer fate detection) algorithm, which detects changes and metabolic fluxes derived from labeled tracers in the primary metabolome. For LC−HRMS-based tracer metabolization approaches, several software tools designed for the untargeted detection and analysis of isotope patterns of metabolites derived from native and partly isotopically labeled tracers are available (e.g., mzMatch-ISO,[10] X^{13}CMS[11]). However, to the best of our knowledge, no tools for the automated global and highly selective detection of only those metabolites derived from native and labeled tracers with nonoverlapping isotope patterns are currently available.

Thus, a LC−HRMS-based workflow for the unbiased detection of known and unknown metabolites derived from U-^{13}C-SIL guided tracer metabolism was developed. It is based on our recently published workflow for the detection of metabolic features derived from native and fully labeled biological samples,[12] which has been further developed to support fast polarity switching and automated annotation of metabolic features of the detected metabolites. In contrast, to the currently existing workflows, such as mzMatch-ISO or fluxomics applications, which have been designed to detect shifts of relative abundances in native isotope patterns, the presented approach requires distinct, nonoverlapping isotope patterns and is capable of detecting metabolites for which the native and labeled analogues differ by ≥4 u. Therefore, it is mainly suited to study the secondary metabolism of a biological system of interest rather than to support the elucidation of primary metabolism. Moreover, the use of nonoverlapping isotope patterns enables determining the exact number of incorporated carbon atoms of the employed tracer in the respective biotransformation product and thus improves sum formula and metabolite annotation. At a less advanced stage, the presented concept has already been used successfully to study the metabolic fate of the mycotoxin deoxynivalenol (DON) in wheat (*Triticum aestivum*, Kluger et al.[13]) and the fate of the aromatic amino acid phenylalanine in grape berries (*Vitis vinifera*, Chassy et al.[14]). Here, our approach is presented with the metabolism of the endogenous amino acid phenylalanine in wheat cell suspension cultures in the presence or absence of the *Fusarium* virulence factor DON. Phenylalanine was chosen as a tracer because it serves as precursor for the biosynthesis of hydroxycinnamic acids, phenylpropanoids, and flavonoids in plants, many of which are known to be involved in the defense against fungal pathogens such as *Fusarium*.[15]

MATERIALS AND METHODS

Chemicals. Acetonitrile (ACN, HiPerSolv Chromanorm, HPLC gradient grade) was purchased from VWR (Vienna, Austria), methanol (MeOH, LiChrosolv, LC gradient grade) was purchased from Merck (Darmstadt, Germany), and formic acid (FA, MS grade) was obtained from Sigma-Aldrich (Vienna, Austria). Water was purified successively by reverse osmosis and an ELGA Purelab Ultra-AN-MK2 system (Veolia Water, Vienna, Austria). U-$^{13}C_9$ phenylalanine (U-$^{13}C_9$ Phe; 99.1% ^{13}C) was purchased from Euriso-top (Saarbrücken, Germany).

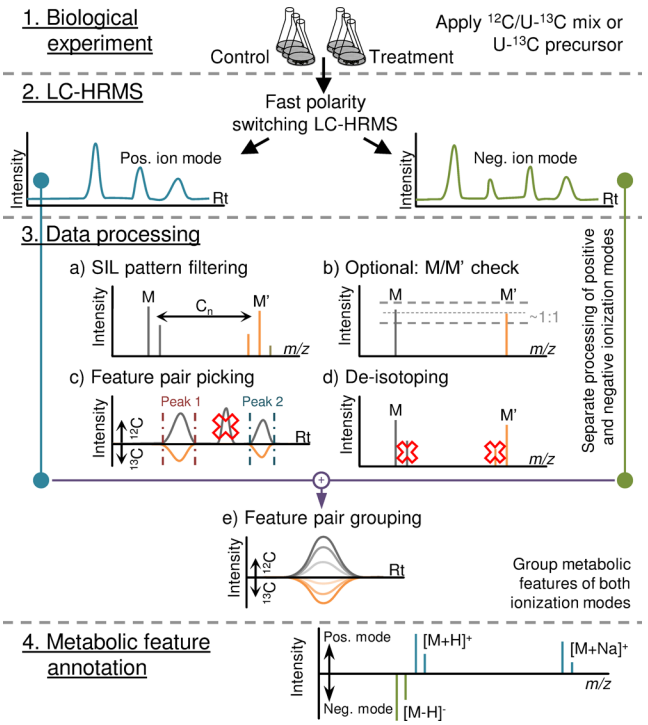

Figure 1. Illustration of the workflow for SIL-assisted tracer metabolism studies, including LC−ESI-HRMS fast polarity switching.

Biological Experiment (Figure 1, Step 1). Aliquots (3.6 mL) of *T. aestivum* (*Tae*) cell suspension cultures in B5 medium (Supporting Information S1.1) were incubated with 400 μL of aqueous solutions differing in composition according to the three tested conditions (3 replicates per condition). Thus, each culture sample resulted in a final volume of 4 mL. For the condition "control", 200 μL of U-$^{13}C_9$ Phe stock solution (final concentration in culture: 25 mg/L) and 200 μL of H_2O dist. were added to the culture. For cocultivation with DON (condition "treatment"), 200 μL of U-$^{13}C_9$ Phe stock solution (final concentration in culture: 25 mg/L) and 200 μL of DON stock solution (final concentration in culture: 90 mg/L) were added. For the condition "blank" 400 μL of H_2O dist. was added to 3.6 mL of cell suspension culture. All *Tae* cell suspension cultures were grown in 25 mL Erlenmeyer flasks for 8 days at 20 °C in the light with shaking (100 rpm). In addition, two medium blanks without cell suspension cultures were prepared in parallel.

Sample Preparation. After cultivation, 2 mL of each sample was transferred into savelock Eppendorf tubes and centrifuged for 5 min at 5000*g*. The weight of each cell pellet was determined, and 350 μL MeOH and 2 × 5 mm steel balls

dx.doi.org/10.1021/ac503290j | *Anal. Chem.* 2014, 86, 11533−11537

were added prior to wet milling with a ball mill (MM 301 Retsch, Haan, Germany). Samples were homogenized for 2 min at 30 Hz, and the suspension was transferred to new Eppendorf tubes and centrifuged for 5 min at 20 000*g*. From the resulting extract, 200 μL was mixed with 200 μL of H_2O dist. and centrifuged for 10 min at 20 000*g* again. An aliquot of 300 μL of this sample solution was transferred to an HPLC vial and stored at −80 °C until further analysis.

LC−HRMS Analysis (Figure 1, Step 2). All samples were analyzed on a UHPLC system (UltiMate 3000, Dionex) coupled to an Orbitrap Exactive Plus (Thermo Fisher Scientific) equipped with a heated electrospray ionization (ESI) source. A Dionex autosampler was used for the injection of 10 μL per sample for chromatographic separation at 25 °C on a reversed-phase XBridge C18 150 × 2.1 mm i.d., 3.5 μm column (Waters, Milford, MA, USA) preceded by a C18 4 × 3 mm i.d. security cartridge (Phenomenex, Torrance, CA, USA). At a constant flow rate of 250 μL/min, a linear gradient program with water containing 0.1% FA (v/v) (eluent A) and MeOH containing 0.1% FA (v/v) was employed;[12] the initial mobile phase composition (10% eluent B) was held constant for 2 min, followed by a linear gradient to 100% eluent B within 30 min. After a hold time of 5 min, the column was re-equilibrated for 8 min at 10% eluent B.

The heated ESI interface was operated in fast polarity-switching mode using the following settings for both polarities: sheath gas, 50 au; auxiliary gas, 5 au; capillary voltage, 3 kV; capillary temperature, 350 °C. FT-Orbitrap was operated in profile mode (scan range, m/z 100−1000) with a resolving power of 70 000 fwhm (at m/z 200) and automatic gain control setting of 3×10^6 with a maximum injection time of 200 ms.

SIL-Assisted Data Processing (Figure 1, Steps 3 and 4). The SIL-assisted data processing for metabolite detection in full metabolome labeling experiments described earlier[12] was extended to support the detection of tracer-derived metabolites. It is part of a software package that is currently under development and will comprise three different data processing workflows for SIL-assisted metabolomics approaches. In the meantime, the software module facilitating data processing according to the presented workflow is accessible via the corresponding author.

Each of the following data processing steps for metabolic feature detection is carried out independently for the positive and negative ionization mode: First, every MS scan is inspected for pairs of two mass peaks, M, which corresponds to a native metabolization product, and M′, which denotes the same metabolization product but contains the labeled tracer molecule or a part of it, with an m/z difference proportional to the number of tracer-derived heavy isotope atoms (here, ^{13}C) present in the labeled metabolite ion (step 3a). A peak pair is accepted if the observed mass difference is within a preset maximum mass tolerance window of that calculated for the algorithm-predicted number of heavy isotopes. Optionally, for exogenous tracers, the intensity ratio I_M:$I_{M'}$ is compared with that of the concentration ratio of native and labeled tracer used for sample incubation (step 3b).

Next, the observed isotopolog ratio $I_{M'-1}/I_{M'}$ is compared with its theoretical ratio expected from the number of labeling isotopes contained in the inspected metabolite ion (step 3a). The corrected intensity ratio of the isotopologs $I_{M+1}/I_M - I_{M'+1}/I_{M'}$, which accounts for any carbon atom in the nonlabeled moiety, is compared with its theoretical ratio as determined for the number of labeling isotopes of the respective M and M′ ion pair. All intensity ratio checks are passed if the relative deviation between the expected and the observed ion intensity ratios are within preset error windows. Then, all such detected M and M′ pairs from different scans are combined with hierarchical clustering using the assigned number of heavy isotopes per metabolite ion and the m/z value of M. Clusters showing a maximum relative mass deviation between their highest and lowest m/z value of less than a preset threshold in parts per million are not further split.

Next, for each M and M′ ion cluster, chromatographic peaks in the corresponding $^{12}C/^{13}C$ EICs are extracted with the wavelet algorithm of Du et al.[16](step 3c). Only those EIC peaks that are found for both ^{12}C and corresponding ^{13}C m/z traces closely coelute and have a high Pearson correlation coefficient remain for further data processing. Incorrectly detected M and M′ pairs that originate from carbon isotopologs (e.g., M + 1 instead of M or M′ − 1 instead of M′) are removed from the data (step 3d). Correctly assigned chromatographic peak pairs are finally listed as metabolic features, each consisting of a ^{12}C monoisotopic m/z for M, a retention time (t_R), feature areas determined for the EIC peaks of M and M′, and the number of heavy isotopes originating from the tracer.

Following metabolic feature detection, all features found in positive or negative ionization mode are combined across both ionization polarities to generate feature groups, each of which represents a distinct metabolite (step 3e). To this end, the Pearson correlation coefficient is calculated pairwise for closely coeluting metabolic features. All metabolic features with a correlation coefficient above a preset threshold are put into the same feature group.

Subsequently, each determined feature group is annotated (step 4). For this, all features of a feature group are inspected pairwise for m/z differences corresponding to predicted ion species frequently found for the respective ionization mode. For metabolic features without a valid adduct pairing, neutral losses are calculated according to the Seven Golden Rules.[17]

LC−HRMS data derived from wheat cell suspension culture samples were processed as described above with the following parameter settings: (step 3a) Isotopic carbon enrichment, 98.9% ^{12}C; 99.1% $^{13}C_9$-Phe; Δ m/z $^{12}C/^{13}C$, 1.00335 u; atom counts, 6−9; minimum intensity threshold of putative M and M′ signals, 50 000 counts; maximum mass deviation between M and putatively corresponding M′ signals, ±3 ppm; maximum isotopolog ratio error, 20%. (step 3c) EIC m/z width, ± 5 ppm; minimum correlation coefficients between EIC peaks of M and M′, 0.75 for peak picking and 0.9 for feature grouping (step 3e). (step 4) Adducts used for feature annotation, $[M + H]^+$, $[M + Na]^+$, $[M + NH_4]^+$, $[M + K]^+$, $[M - e]^+$, $[M - H]^-$, $[M + FA - H]^-$, $[M + Na - 2H]^-$, $[M + Cl]^-$, $[M + K - 2H]^-$, $[M + Br]^-$, $[M - e - 2H]^-$. The accurate m/z values of all detected metabolites were searched against a custom wheat metabolite database containing 1145 entries (max m/z difference ≤ 5 ppm). Statistical evaluation of the experiment is described in Supporting Information S1.3.

RESULTS AND DISCUSSION

In a biological system, native and ^{13}C-enriched substances are metabolized by the same biological transformations and to a nearly equal extent.[6] As a result, all metabolites derived from a mixture of native and ^{13}C-labeled tracer contain either the entire native or the enriched tracer or just a part of it. In LC−HRMS, native metabolites and their corresponding ^{13}C isotopologs perfectly coelute with highly similar chromato-

dx.doi.org/10.1021/ac503290j | Anal. Chem. 2014, 86, 11533−11537

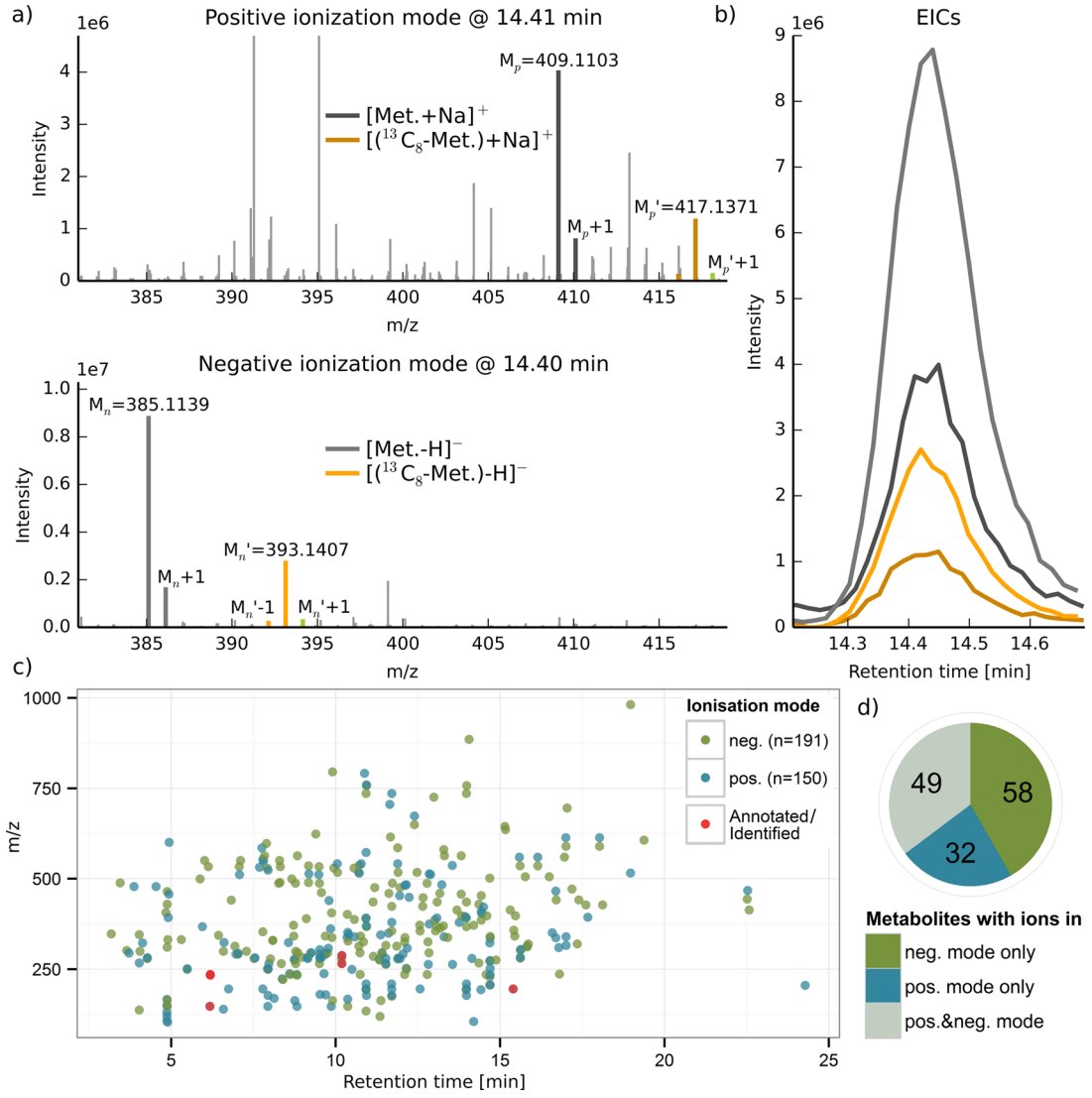

Figure 2. (a, b) Illustration of two metabolic feature pairs detected for the same metabolite. (a) Two mass spectra derived from positive and negative ionization mode for the respective native and corresponding $^{13}C_8$-labeled features derived from phenylalanine. (b) EIC profiles of the respective metabolic features shown in part a. (c) m/z versus retention time plot of all $^{13}C_9$-Phe-derived features detected in the positive and negative ionization mode and (d) their convolution into a feature group. The red dots represent selected metabolic features from three of the either annotated or identified metabolites. For details, see Supporting Information S1.2.

graphic peak shapes but can be easily distinguished by MS because of their differing m/z values. The observed m/z shift between the native and the partly tracer-labeled biotransformation product is proportional to the number of atoms of the labeling isotope in the remaining part of the tracer of the inspected metabolite ion. The presented workflow automatically searches for these unique isotope patterns and returns a comprehensive list of metabolic features, each corresponding to an ion of a metabolite derived from the studied tracer. As long as the isotope patterns of the tracer(s) incorporated in the respective metabolite can be separated, the algorithm can detect all metabolic feature pairs of a biotransformation product, including those isotopologs originating from the incorporation of different tracer moieties. The SIL-derived isotope patterns provide a high certainty that the detected metabolites are truly derived from the studied tracer.

To demonstrate the workflow, the metabolic fate of the amino acid phenylalanine (Phe) was studied in *Tae* cell suspensions cultured in the presence of U-$^{13}C_9$ Phe in the culture medium. Processing of the acquired raw data resulted in a total of 341 metabolic features, which were convoluted to 139 feature groups, each of which is representing a metabolite. Figure 2a shows two mass spectra containing a metabolism product with eight tracer-derived carbon atoms (native M) and its partly ^{13}C-labeled analog M′. The presence of the M′ + 1 mass peaks indicate that the moiety conjugated to the tracer also contains several carbon atoms.

Two medium blanks and *Tae* cell suspension cultures (no U-$^{13}C_9$ Phe added) were processed as described above. Only 1−2 of incorrectly detected metabolic features were found per sample, which during manual curation showed to be Fourier transformation artifacts with low abundances and noisy chromatographic peak shapes. This very low number of false positives confirms the high selectivity of the presented SIL assisted approach.

Fast Polarity Switching. The presented workflow supports fully automated processing of LC−ESI-HRMS data employing fast polarity switching. The cycle time for two successive MS

dx.doi.org/10.1021/ac503290j | *Anal. Chem.* 2014, 86, 11533−11537

scans (positive and negative ionization mode) was ∼1 s, which is sufficient to acquire 10−25 scans per chromatographic peak. As shown in Figure 2b, the chromatographic peak shapes are very similar for all four depicted mass traces (of M_p, M_p', M_n, M_n'); thus, even features originating from the same metabolite but recorded in different ionization modes can be convoluted automatically into a single feature group.

In the presented experiment, 150 and 191 metabolic features were detected in the positive and negative ionization modes, respectively (Figure 2c). Furthermore, feature grouping across the two ion polarity modes was carried out successfully and resulted in a total of 139 distinct feature groups (i.e., metabolites). Of those, 32 were exclusively found in the positive mode, and 58 metabolites were detected in the negative ionization mode only. In addition, 49 metabolites exhibited at least one metabolic feature in each of the both ionization modes (Figure 2d). These findings underline the significant benefit that has been gained with respect to metabolite coverage by integrating positive and negative mode data.

Metabolite Annotation. The presented workflow results in a list of metabolic features, each corresponding to a certain ion species (e.g., adduct, deprotonated molecule, or in-source fragment) of a metabolite. For 19 of the 49 detected phenylalanine-derived metabolites with complementary adducts from both ionization modes, annotation of their intact neutral molecule and, thus, the corresponding molecular weight was achieved only by integration of ion species related information from the respective opposite ionization mode. This further demonstrates the power of fast polarity switching for complementary metabolite annotation.

The database search revealed that 50 of the detected metabolites, several with the same molecular mass, were putatively annotated. Although metabolite annotation was not always unambiguous, the metabolites could be assigned to phenylpropanoids (n = 14), phenylpropanoid amides (n = 9), and flavonoids (n = 10), which are partly known to have antagonistic effects against *Fusarium* infection (Supporting Information S1.2). Detailed metabolite annotation and biological interpretation of results will be published elsewhere.

DON Treatment. After data processing with the developed workflow, hierarchical clustering analysis (HCA) showed two distinct clusters for the two conditions "control" and "treatment". Furthermore, the heatmap illustration indicates that the abundance of many metabolites is either increased or decreased in the DON-treated samples. This confirms that the DON treatment had a severe impact on the cells metabolic composition (Supporting Information S1.3).

CONCLUSION

In recent years, SIL has been increasingly used in many fields of targeted and untargeted metabolomics research. The presented SIL-assisted LC−HRMS-based workflow is well suited to study the metabolic fate of both endogenous and exogenous tracer substances. All metabolites derived from the studied native and ^{13}C-labeled tracers show unique isotope patterns, which enable their untargeted detection and provide high confidence that the detected metabolites are truly derived from the studied tracer substance. The presented approach is particularly suited for the investigation of secondary metabolism and can be applied to virtually any biological system without the need for extra equipment other than the labeled tracer compound(s). As demonstrated for wheat cell suspension cultures, the use of ESI in combination with fast polarity switching, the study of endogenous plant secondary metabolite precursors (for example, phenylalanine) directly results in a large number of complementary Phe-related metabolic features, which can be assigned to various structure classes. In conclusion, our data demonstrate the great potential of SIL-assisted workflows for the comprehensive and highly selective untargeted screening and annotation of metabolites truly derived from the studied tracer. The workflow supports valuable applications across many different fields of metabolomics research, such as drug, pesticide, toxin, or any other secondary metabolite precursor-related conversion. A software tool and technical assistance enabling the fully automated processing according to the presented strategy are available from the corresponding author. Moreover, this software tool will be published and made freely available as part of an even more comprehensive software package for the evaluation of SIL-derived metabolomics data in the near future.

ASSOCIATED CONTENT

Supporting Information

Additional information as noted in the text. This material is available free of charge via the Internet at http://pubs.acs.org

AUTHOR INFORMATION

Corresponding Author

*E-mail: rainer.schuhmacher@boku.ac.at.

Author Contributions

¶B.K. and C.B. contributed equally to this work.

Notes

The authors declare no competing financial interest.

ACKNOWLEDGMENTS

The authors thank Denise Schöfbeck, Sylvia Lehner, and Benedikt Warth for useful discussions. The Austrian Science Fund (SFB-Fusarium-3706-B11;3702) and the Austrian Ministry of Science and Research (OMICS Center Graz) are acknowledged for financial support.

REFERENCES

(1) Levsen, K.; et al. *J. Chromatogr., A* **2005**, *1067* (1−2), 55−72.
(2) Sandermann, H. *Pest Manage. Sci.* **2004**, *60* (7), 613−623.
(3) Zhang, H.; et al. *J. Mass Spectrom.* **2008**, *43* (9), 1191−200.
(4) Baillie, T. A. *Pharmacol. Rev.* **1981**, *33* (2), 81−132.
(5) Iglesias, J.; Sleno, L.; Volmer, D. A. *Curr. Drug Metab.* **2012**, *13* (9), 1213−1225.
(6) Klein, S.; Heinzle, E. *Wiley Interdiscip. Rev.: Syst. Biol. Med.* **2012**, *4* (3), 261−272.
(7) Cabaret, O.; et al. *Rapid Commun. Mass Spectrom.* **2011**, *25* (19), 2704−10.
(8) Li, F.; et al. *J. Proteome Res.* **2013**, *12* (3), 1369−1376.
(9) Hiller, K.; et al. *Bioinformatics* **2013**, *29* (9), 1226−1228.
(10) Chokkathukalam, A.; et al. *Bioinformatics* **2013**, *29* (2), 281−283.
(11) Huang, X.; et al. *Anal. Chem.* **2014**, *86* (3), 1632−1639.
(12) Bueschl, C.; et al. *Metabolomics* **2014**, *10*, 754−769.
(13) Kluger, B.; et al. *Anal. Bioanal. Chem.* **2013**, *405* (15), 5031−6.
(14) Chassy, A. W.; et al. *Food Chem.* **2015**, *166* (0), 448−455.
(15) Gunnaiah, R.; Kushalappa, A. C. *Plant Physiol. Biochem.* **2014**, *83C*, 40−50.
(16) Du, P.; Kibbe, W. A.; Lin, S. M. *Bioinformatics* **2006**, *22* (17), 2059−2065.
(17) Kind, T.; Fiehn, O. *BMC Bioinf.* **2007**, *8* (1), 105.